blood advances

American Society of Hematology
2021 L Street NW, Suite 900,
Washington, DC 20036
Phone: 202-776-0544 | Fax 202-776-0545
bloodadvances@hematology.org

Deleting ACC1 in platelets alters phospholipidome and reduces platelet activation and thrombosis in mice

Tracking no: ADV-2025-015796R2

Marie octave (Université catholique de Louvain, Belgium) Laurence Pirotton (UCLouvain, Belgium) Emma de Cartier d'Yves (Université catholique de Louvain, Belgium) Alice Marino (Université catholique de Louvain, Belgium) Jérôme Ambroise (Université catholique de Louvain, Belgium) Martin Giera (Leiden University Medical Center, Netherlands) Bruno Guigas (Leiden University Medical Center, Netherlands) Audrey Ginion (UCL, Belgium) Valentine Robaux (UCLouvain, Belgium) Marijke Kuijpers (Maastricht University Medical Centre, Netherlands) Constance Baaten (University Hospital RWTH Aachen, Germany) Johan Heemskerk (Synapse Research Institute, Netherlands) Zoltan Nagy (University Hospital WÃ¼rzburg, Germany) Yotis Senis (Etablissement Francais du Sang Grand-Est, France) Davide Brusa (Université catholique de Louvain, Belgium) Caroline Bouzin (UCLouvain, Belgium) Luc Bertrand (UCLouvain, Belgium) Christophe Beauloye (Cliniques universitaires Saint-Luc, Belgium) Sandrine Horman (Université catholique de Louvain, Belgium)

Abstract:
This study uncovers the pivotal role of acetyl-CoA carboxylase 1 (ACC1) in regulating platelet lipid composition, bioenergetics, activation, and thrombus formation, as demonstrated using a targeted GPIbα-Cre+/- mouse model. By comparing platelet-specific ACC1 knockout mice (pKO; GPIbα-Cre+/- x ACC1flx/flx) with both GPIbα-Cre+/- and ACC1flx/flx control groups, we showed that ACC1 deficiency profoundly reshaped the platelet phospholipidome. Specifically, ACC1 deletion led to decreased levels of arachidonic acid-containing phosphatidylethanolamine plasmalogens, thereby limiting thromboxane A2 synthesis, dense granule secretion, and platelet activation upon agonist stimulation. Bioenergetic analysis of ACC1-deficient platelets revealed reduced glycolytic activity, potentially worsening their activation defects. Notably, ACC1 deficiency also enhanced the mitochondrial reserve respiratory capacity, without altering basal respiration or ATP turnover. This increased reserve respiratory capacity correlated with reduced phosphatidylserine exposure, suggesting lower procoagulant activity. Importantly, we showed that ACC1 deficiency impaired thrombus formation without compromising hemostasis. Together, these findings identified ACC1 as a critical regulator of platelet function and highlighted its potential as a target for innovative anti-thrombotic therapies.

Conflict of interest: No COI declared

COI notes:

Preprint server: No;

Author contributions and disclosures: M.O. and L.P. performed the experiments, analyzed the data, wrote and edited the manuscript; E.D. wrote and edited the manuscript; A.M. performed the experiments, acquired and analyzed the data, especially for the arterial thrombosis studies; J.A. carried out the biostatistical and lipidomic data analysis; M.G. and B.G. performed the experiments, acquired and analyzed the data, especially for the lipidomic studies; A.G. and V.R. performed the experiments, acquired and analyzed the data, especially for flow cytometry analyses; M.K., C.Ba. and J.W.M.H. performed the experiments, acquired and analyzed the data, especially for the flow chambers studies; Z.N. and Y.S. generously provided the GpIb□-Cre animals mice; D.B. and C.Bo. provided experimental and conceptual advice on flow cytometry and immunohistochemistry experiments, respectively; L.B. secured funding, discussed results and their implications, and edited the manuscript; C.Be. conceived and designed the study, secured funding, discussed results and their implications and edited the manuscript. S.H. conceived and designed the study, secured funding, discussed results and their implications, wrote and edited the manuscript.

Non-author contributions and disclosures: No;

Agreement to Share Publication-Related Data and Data Sharing Statement: The dataset will be made available upon request through contact with the corresponding author.

Clinical trial registration information (if any):

Title

Deleting ACC1 in platelets alters phospholipidome and reduces platelet activation and thrombosis in mice

Short Title

ACC1 modulates platelet lipids and function

Authors and affiliations

Marie Octave[1$], Laurence Pirotton[1$], Emma de Cartier d'Yves[1], Alice Marino[1], Jérôme Ambroise[2], Martin Giera[3], Bruno Guigas[4], Audrey Ginion[1], Valentine Robaux[1], Marijke Kuijpers[5,6], Constance Baaten[5,7], Johan W M Heemskerk[5], Zoltan Nagy[8], Yotis Senis[9], Davide Brusa[10], Caroline Bouzin[11], Luc Bertrand[1], Christophe Beauloye[1,12,13], Sandrine Horman[1*]

[1]Pôle de Recherche Cardiovasculaire (CARD), Institut de Recherche Expérimentale et Clinique (IREC), Université catholique de Louvain (UCLouvain), Brussels, Belgium

[2]Centre de Technologies Moléculaires Appliquées, Institut de Recherche Expérimentale et Clinique, UCLouvain, Brussels, Belgium

[3]Department of Molecular Cell Biology, Leiden University Medical Center, Leiden, The Netherlands

[4]Leiden University Center for Infectious Diseases (LUCID), Leiden University Medical Center, Leiden, The Netherlands

[5]Department of Biochemistry, Cardiovascular Research Institute Maastricht (CARIM), Maastricht University, Maastricht, The Netherlands

[6]Thrombosis Expertise Centre, Heart and Vascular Centre, Maastricht University Medical Centre, Maastricht, The Netherlands

[7] Institute for Molecular Cardiovascular Research (IMCAR), University Hospital RWTH Aachen; Aachen, Germany

[8]Institute of Experimental Biomedicine, University Hospital and Rudolf Virchow Center, University of Würzburg, Würzburg, Germany

[9]Institut National de la Santé et de la Recherche Médicale (INSERM), Etablissement Français du Sang Grand Est, Unité Mixte de Recherche (UMR) S1255, Fédération de Médecine Translationnelle de Strasbourg, Université de Strasbourg, Strasbourg, France

[10]CytoFlux-Flow Cytometry and Cell Sorting Plateform, IREC, UCLouvain, Brussels, Belgium

[11]IREC Imaging Plateform (2IP - RRID:SCR_023378), IREC, UCLouvain, Brussels, Belgium

[12]Department of Cardiology, Cliniques universitaires Saint-Luc, Brussels, Belgium

[13]Department of Cardiovascular Intensive Care, Cliniques universitaires Saint-Luc, Brussels, Belgium

[$]Contributed equally and are joint first authors

***Corresponding author**

Prof. Sandrine Horman, PhD

Pôle de Recherche Cardiovasculaire, Institut de Recherche Expérimentale et Clinique (IREC), UCLouvain

Avenue Hippocrate, 55 (B1.55.05)

1200 Brussels, Belgium

Tel: +32 2 764 5566

Email: sandrine.horman@uclouvain.be

Data sharing statement

The dataset will be made available upon request through contact with the corresponding author.

Text: 3982 words

Abstract: 162 words

Figures: 7

Supplemental Figures: 5

Supplemental Tables: 2

References: 65

Key Points

- Lipidomic analysis combined with a knockout mouse model identified ACC1 as a key regulator of the platelet lipidome
- Phospholipid pools regulated by ACC1 are essential for platelet metabolism and activation

Abstract

This study uncovers the pivotal role of acetyl-CoA carboxylase 1 (ACC1) in regulating platelet lipid composition, bioenergetics, activation, and thrombus formation, as demonstrated using a targeted GPIbα-Cre$^{+/-}$ mouse model. By comparing platelet-specific

ACC1 knockout mice (pKO; GPIbα-Cre$^{+/-}$ x ACC1$^{flx/flx}$) with both GPIbα-Cre$^{+/-}$ and ACC1$^{flx/flx}$ control groups, we showed that ACC1 deficiency profoundly reshaped the platelet phospholipidome. Specifically, ACC1 deletion led to decreased levels of arachidonic acid-containing phosphatidylethanolamine plasmalogens, thereby limiting thromboxane A_2 synthesis, dense granule secretion, and platelet activation upon agonist stimulation. Bioenergetic analysis of ACC1-deficient platelets revealed reduced glycolytic activity, potentially worsening their activation defects. Notably, ACC1 deficiency also enhanced the mitochondrial reserve respiratory capacity, without altering basal respiration or ATP turnover. This increased reserve respiratory capacity correlated with reduced phosphatidylserine exposure, suggesting lower procoagulant activity. Importantly, we showed that ACC1 deficiency impaired thrombus formation without compromising hemostasis. Together, these findings identified ACC1 as a critical regulator of platelet function and highlighted its potential as a target for innovative anti-thrombotic therapies.

Keywords

Platelet, Acetyl-CoA carboxylase, *de novo* lipogenesis, Lipidome, Glycerophospholipids, Arachidonic acid, Thromboxane, Thrombosis, Hemostasis

Introduction

Understanding the role of lipid composition in the platelet plasma membrane is crucial for unraveling hemostasis and thrombosis complexity. Lipids significantly influence platelet functionality, membrane fluidity, curvature, shape changes, and bioactive signaling molecule production.[1-7] Several lipidomic studies have characterized lipid profiles of both resting and activated platelets[4, 8-13], identifying glycerophospholipids - including phosphatidylcholine (PC), phosphatidylethanolamine (PE), phosphatidylserine (PS), and phosphatidylinositol (PI) - as the main lipid class.[10] These glycerophospholipids differ in their head groups as well as

length and saturation of their two fatty acyl chains.[1, 6, 14] Watanabe *et al.* reported that the main saturated fatty acids in the platelet plasma membrane are palmitic acid (PAL, 16:0) and stearic acid (SA, 18:0), with oleic acid (OA, 18:1) and arachidonic acid (AA, 20:4) being the predominant unsaturated fatty acids.[15] Arachidonic acid is particularly abundant in phosphatidylethanolamine plasmalogen (PEP), a glycerophospholipid subclass characterized by a vinyl-ether bond at the sn-1 position of the glycerol backbone.[1] Upon platelet activation, these arachidonylated plasmalogens are selectively hydrolyzed by the phospholipase A_2 (PLA_2), releasing AA and generating lysophospholipid species.[16-18] Subsequent AA oxidation via the cycloxygenase and lipoxygenase pathways produces key lipid mediators, such as thromboxane A_2 (TxA_2) and other eicosanoids, which are crucial for platelet activation and bioenergetics.[4, 6, 19-21]

Platelets can synthesize lipids and fatty acyls *de novo.*[22, 23] Acetyl-Coenzyme A (CoA) carboxylase (ACC) has emerged as a key enzyme in this process, catalyzing malonyl-CoA production, the rate-limiting substrate for *de novo* lipogenesis (DNL).[24] Among the two isoforms (ACC1 and ACC2), ACC1 is the predominant isoform in platelets.[20, 25, 26] While DNL is typically considered a moderate contributor to intracellular lipid stores, a modulation of DNL can significantly alter membrane lipid saturation and the properties of various cell types, including endothelial [27] and cancer cells.[28, 29] We have previously demonstrated that systemic AMPK-ACC signaling inhibition and the resulting sustained ACC activation modifies AA-containing PEP levels in platelets, thereby influencing their reactivity to collagen and promoting thrombosis through increased TXA_2 generation.[20] Recent studies have also linked ACC to demarcation membrane formation in megakaryocytes (MKs), which is crucial for platelet biogenesis.[30] However, whether platelets derived from ACC-deficient MKs exhibit altered lipidome composition, reduced activation or functional impairments remains unknown. In this study, we investigated the impact of ACC1 deletion on platelet lipid composition and function. Using GPIbα-Cre$^{+/-}$ mice for platelet-specific genetic ACC1 deletion, we demonstrated that ACC1 is essential for regulating the PEP lipid class and the overall levels

of saturated and long polyunsaturated fatty acyl chains in platelet glycerophospholipids. These regulatory mechanisms directly impacted platelet functionality, resulting in reduced thrombosis in mice. Our findings suggest that targeting DNL or ACC1 could be a promising strategy to prevent thrombotic disorders.

Methods

Additional materials and methods are outlined in the supplemental data.

Mice

Platelet-specific ACC1 knockout mice were generated by crossing $ACC1^{flx/flx}$ females (Jackson laboratory) with GPIbα-$Cre^{+/-}$ males [31], yielding $ACC1^{flx/flx}$ X GpIbα-$Cre^{+/-}$ mice and $ACC1^{flx/flx}$ control mice. GpIbα-$Cre^{+/-}$ animals were used as additional controls. All mice were on a C57BL/6 background, males aged 8–16 weeks, and maintained on standard chow diet. Animal experiments followed ARRIVE guidelines and were approved by local ethics committees (Comité d'éthique facultaire pour l'expérimentation animale, 2016/UCL/MD/027 and 2021/UCL/MD/012).

Lipidomics

Platelets ($2x10^8$) were suspended in modified Tyrode's buffer with 0.35% free fatty acid bovine serum albumin (BSA). Dry platelet pellets were obtained by centrifugation at 11,700g for 15 seconds, then stored at -80°C prior to lipid extraction. Lipid extraction and subsequent lipidomic analysis were conducted as previously described.[1]

Lipidomic data statistical analysis

Lipid species concentrations were analyzed using R.4.2.1 according to the following bioinformatics pipeline. The lipid species concentration matrix and associated metadata were imported into a SummarizedExperiment object (v.1.28.0), and lipid species with >80% missing values were excluded. Normalization was performed via the MSTUS method, followed by log2 transformation. Linear models for each lipid species were built using limma (v3.54.2), yielding fold changes and p-values, which were FDR-adjusted (Benjamini-

Hochberg, FDR≤0.05). Visualizations were produced using ggplot2 (v3.4.2), ggradar (v0.2), and forestplot (v3.1.1).

Statistical analysis

Statistical parameters including sample size, mean, standard error of the mean (SEM), and statistical significance are specified in the figure legends. P-values≤0.05 were considered statistically significant. Statistical analyses were performed using GraphPad Prism 9.1.2 (GraphPad Software, San Diego, CA).

Results

Platelet-specific ACC1 knockout mice displayed reduced platelet counts and increased αIIbβ3 expression

We developed a platelet-specific ACC1 knockout (pKO) mouse model and confirmed the absence of ACC1 expression in platelets, with no compensatory ACC2 upregulation (Figure 1A). ACC1 expression levels in leukocytes from ACC1 pKO mice were comparable to those from $ACC1^{flx/flx}$ and GPIbα-$Cre^{+/-}$ control mice, confirming the specificity of the ACC1 floxed gene deletion within the MK lineage by GPIbα-Cre-mediated recombination. Liver extracts were used as positive controls for detecting both ACC1 and ACC2. ACC1 deficiency resulted in a significant platelet count reduction compared with $ACC1^{flx/flx}$ and GPIbα-$Cre^{+/-}$ control mice, along with a platelet volume increase (Figure 1B and C). Minor changes were noted in other blood cell types, including erythrocytes, leukocytes, lymphocytes, and granulocytes, with hematocrit levels remaining similar across all three genotypes, suggesting that these effects were platelet-specific (supplemental Table 1). Flow cytometry analysis of platelets isolated from mice injected with Alexa488-GPIbβ antibodies revealed a modest but significant reduction in platelet clearance in ACC1-deficient mice compared to both $ACC1^{flx/flx}$ and GPIbα-$Cre^{+/-}$ control groups three days after injection, indicating that the reduced platelet counts observed in ACC1 pKO mice is not due to increased platelet turnover (supplemental

Figure 1A, Figure 1D). Given the role of CD36 in megakaryopoiesis [30, 32, 33], we assessed its expression in ACC1-deficient platelets as a read-out for potential changes in megakaryocytes. CD36 levels were increased in ACC1 pKO platelets compared to both controls (supplemental Figure 1E), arguing against CD36 downregulation as a cause of the observed thrombocytopenia.

Further flow cytometry analysis of major platelet surface receptors, normalized to mean platelet volume (MPV), revealed a modest increase in αIIbβ3 expression in ACC1 pKO compared with ACC1$^{flx/flx}$ and GPIbα-Cre$^{+/-}$ platelets (Figure 1E). In contrast, the expression levels of other receptors, such as GPIbα or GPVI, were not elevated in ACC1-deficient platelets. Interestingly, GPIbα expression was even reduced in GPIbα-Cre$^{+/-}$ platelets, compared with both ACC1$^{flx/flx}$ and ACC1 pKO platelets (Figure 1E), despite a slightly increased platelet volume. This reduction in GPIbα expression has been previously documented in GPIbα-Cre$^{+/-}$ mice.[31] Finally, Western blot analysis of PAR3, PAR4, and TP receptors showed comparable expression levels across the three genotypes, with no consistent or statistically significant differences observed (supplemental Figure 1B-D).

Lipidomic analysis revealed distinct changes in lipid profiles of ACC1 pKO platelets

To investigate the impact of ACC1 deficiency on platelet lipid composition, we performed a lipidomic analysis on resting platelets from ACC1 pKO mice and compared the results with those of the two control groups (ACC1$^{flx/flx}$ and GPIbα-Cre$^{+/-}$) using the Lipidyzer platform. Principal component analysis (PCA) was conducted to distinguish the lipidome profiles of ACC1 pKO mice from those of the control groups. The PCA revealed a clear separation between the lipid profiles of ACC1 pKO and control mice, with the two principal components accounting for 50.1% of the variance in the lipidome across the three genotypes (Figure 2A). The lipidomic analysis identified 446 lipid species across 16 lipid classes/subclasses, including fatty acids (FA), diacylglycerol (DG), triacylglycerol (TG), phosphatidic acid (PA), PC, PE, PEP, phosphatidylglycerol (PG), PI, PS, lysophosphatidyl-choline (LPC),

lysophosphatidyl-ethanolamine (LPE), sphingomyelin (SM), ceramide (CER), hydroxyceramide (HCER), and cholesterol ester (CE) when comparing ACC1 pKO with ACC1$^{flx/flx}$ mice. Notably, 168 lipid species (38% of the identified platelet lipid species) were significantly differentially expressed between these two groups (Figure 2B; supplemental Table 2). Similarly, when comparing ACC1 pKO and GPIbα-Cre$^{+/-}$ mice, 206 out of the 436 identified lipid species were differentially expressed (supplemental Figure 2A; supplemental Table 2). Class-wide analysis revealed that ACC1 deficiency led to a down-regulation of PEP species, while CER, PC, and PE lipid classes were up-regulated (Figure 2B; supplemental Figure 2A). To further explore changes in phospholipid species, we examined differences in fatty acyl chain length and unsaturation degree among groups. Consistent with previous studies[20, 27, 28], our analysis revealed that ACC1 deficiency was associated with a decrease in PAL (16:0) across three phospholipid classes (PC, PE, and PEP). In contrast, levels of long polyunsaturated fatty acids (PUFAs) such as AA (20:4), eicosapentaenoic acid (EPA, 20:5), and docosahexaenoic acid (DHA, 22:6) were increased in PC and PE classes (Figure 2C-E**;** supplemental Figure 2B-D). Given that AA is a key precursor for the generation of signaling mediators in platelets, we specifically assessed the levels of AA-containing phospholipids (PC, PE, and PEP) across the three genotypes. Our findings showed that AA-containing PC or PE were up-regulated, whereas AA-containing PEP levels were reduced in ACC1 pKO compared with both ACC1$^{flx/flx}$ and GPIbα-Cre$^{+/-}$ control platelets (Figure 2F; supplemental Figure 2E). A comparative analysis of the relative abundance of AA-containing phospholipids among groups revealed that the PEP 16:0/20:4 species was the most abundant within platelet phospholipid classes in control mice. In ACC1 pKO mice, the PEP 16:0/20:4 species is reduced, and PE 18:0/20:4 becomes the most abundant (Figure 2G; supplemental Figure 2F)**.** Overall, these results underscored the pivotal role of ACC1 in the modulation of both saturated and polyunsaturated fatty acyl chain levels in platelet phospholipids. Notably, arachidonylated plasmalogen regulation may have significant implications for platelet

responsiveness to agonists, potentially by impacting energy metabolism and/or TxA_2 generation.

Energy metabolism was modulated in ACC1 pKO platelets

Given that acyl-CoA, especially AA (20:4) and eicosanoids, serve as substrates for platelet mitochondrial β-oxidation[4, 19], we investigated the impact of ACC1 deficiency on energy metabolism. We initially measured the basal oxygen consumption rate (OCR) and subsequently monitored changes following either thrombin injection (1U/ml) or vehicle (Dulbecco's modified eagle medium; DMEM) over a 30 minutes period. Under non-stimulated conditions, OCR was comparable between control and ACC1 pKO platelets, with glucose as the metabolic substrate. Thrombin injection resulted in a similar OCR increase in ACC1-deficient and control platelets (Figure 3A and B; supplemental Figure 3A and B). To further evaluate oxidative phosphorylation, we injected oligomycin, an adenosine triphosphate (ATP) synthase inhibitor, which led to the anticipated OCR decrease. ATP-linked respiration did not differ significantly between ACC1 pKO and control platelets. Following this, carbonyl cyanide-p-trifluoromethoxyphenylhydrazone (FCCP), a mitochondrial uncoupler that disrupts membrane potential, was used to induce maximal respiration, which was found to be similar among all three genotypes under basal conditions (Figure 3A and B, supplemental Figure 3A and B). Upon thrombin stimulation, there was a decrease in maximal respiration and reserve capacity in $ACC1^{flx/flx}$ and GPIbα-$Cre^{+/-}$ platelets.[4, 34] Interestingly, ACC1 deficiency was associated to a significant increase in mitochondrial respiratory reserve after thrombin stimulation compared with $ACC1^{flx/flx}$ platelets, suggesting a greater availability of endogenous metabolic substrates to meet the increased energetic demand. The same trend was observed in comparison to GPIbα-$Cre^{+/-}$ platelets. Finally, the respiratory-chain complex I/III inhibitors rotenone/antimycin A (R/AtA) reduced mitochondrial-induced OCR to a similar extent across all three genotypes, and proton leak remained unchanged among groups (Figure 3A and B; supplemental Figure 3A and B). In parallel, extracellular acidification rate

(ECAR), which reflects proton release primarily due to lactate production and is commonly used as an indirect indicator of glycolytic activity, increased upon thrombin stimulation in all genotypes. Specifically, thrombin induced an increase in ECAR relative to resting conditions in both control and ACC1 pKO platelets. However, absolute ECAR values remained consistently lower in ACC1-deficient platelets, suggesting reduced glycolytic capacity (Figure 3C and D, supplemental Figure 3C and D). These findings suggest that ACC1 can be involved in the regulation of platelet energy metabolism, a feature that may affect their ability to respond effectively to thrombogenic stimuli.

Reduced arachidonylated PEP content restricted TxA_2 generation and dense granule release in ACC1 pKO platelets

We next evaluated the impact of ACC1 deficiency on TxA_2 production by measuring TxB_2 levels. Platelets lacking ACC1 showed a significant reduction in TxB_2 generation following thrombin and collagen-related peptide (CRP) stimulation. Aspirin was used as a positive control for TxB_2 generation inhibition (Figure 4A). Of note, the observed reduction in TxB_2 production in ACC1 pKO platelets is unlikely to result from impaired phospholipase A_2 (PLA_2) activation, as PLA_2 activity remained comparable between ACC1 and control platelets in both resting and thrombin-stimulated conditions (supplemental Figure 4F). Since TxA_2 acts as a secondary platelet agonist involved in αIIbβ3 integrin activation and dense granule secretion[35], we further examined platelet reactivity to thrombin and CRP. We first investigated αIIbβ3 inside-out signaling by analyzing platelet aggregation. ACC1 pKO platelets displayed reduced aggregation in response to both thrombin and CRP compared with $ACC1^{flx/flx}$ platelets (Figure 4B and C). This impaired aggregation correlated with decreased αIIbβ3 activation, as indicated by the reduced JON/A antibody binding compared with $ACC1^{flx/flx}$ platelets (Figure 4D). We then analyzed platelet granule secretion. Following thrombin stimulation, surface expression of P-selectin, a marker for α-granule secretion, was similar between ACC1 pKO and $ACC1^{flx/flx}$ platelets. However, it tended to be reduced in ACC1 pKO platelets at low CRP concentrations (Figure 4E), suggesting that ACC1

deficiency may modestly impair α-granule secretion in response to this agonist. In contrast, ATP release, indicative of dense granule secretion, was significantly reduced in ACC1 pKO platelets compared with ACC1$^{flx/flx}$ platelets following thrombin or CRP stimulation (Figure 4F and G). Importantly, similar results in TxA_2 generation, platelet aggregation, and dense granule release were observed when comparing platelets from ACC1 pKO mice with those from GPIbα-Cre$^{+/-}$ mice (supplemental Figure 4B-F). These findings highlight the pivotal role of ACC1 in regulating platelet reactivity through the synthesis of AA-containing PEP, used as a source for TxA_2 production. To test whether impaired aggregation could be rescued by supplementing secondary mediators, we co-stimulated ACC1 pKO platelets with thrombin and exogenous ADP. However, this co-stimulation failed to restore aggregation to control levels, suggesting that the functional defect extends beyond impaired ADP release (supplemental Figure 4G and 4H).

Interestingly, the absence of ACC1 also altered platelet morphology under both resting and stimulated conditions. At rest, ACC1-deficient platelets exhibited a significantly larger surface area when spread on fibrinogen (12.58 ± 0.7917 μm²) compared to ACC1$^{flx/flx}$ platelets (9.392 ± 0.5965 μm²) and GPIbα-Cre$^{+/-}$ platelets (10.39 ± 0.712 μm²) (Figure 5A-C). However, upon CRP stimulation, ACC1-deficient platelets displayed a notably reduced proportion of fully spread platelets compared to controls. Instead, a higher number of filopodia-extending platelets was observed, indicating a failure to achieve full spreading under agonist stimulation (Figure 5A, 5D-E).

Platelet-specific ACC1 deletion reduced thrombus formation on collagen-coated surfaces under flow conditions

To evaluate platelet functions under dynamic conditions, we perfused anti-coagulated blood over collagen I- and III-coated surfaces at a shear rate of 1,000s^{-1} and examined thrombus formation. Brightfield images were captured to assess platelet adhesion and thrombus buildup. Platelet adhesion was quantified by analyzing the surface area coverage (SAC),

while thrombus formation was characterized by the surface area covered by multilayered thrombi and thrombus contraction score.[36, 37] Compared with ACC1$^{flx/flx}$ or GPIbα-Cre$^{+/-}$, ACC1 pKO mice blood exhibited decreased platelet adhesion and multilayered thrombus formation, regardless of collagen-coated surface type (Figure 6A-D, supplemental Figure 5A-D). This reduction was likely due to the reduced TxA_2 and adenosine diphosphate (ADP) secretion, which are secondary agonists essential for platelet aggregation on collagen surfaces.[20, 38, 39] Platelet activation in the flow chamber was simultaneously monitored using fluorescently labeled anti-P-selectin antibodies, JON/A antibodies, and annexin V to assess α-granule secretion, αIIbβ3 activation, and PS externalization (reflecting platelet procoagulant activity), respectively. Quantification showed significantly reduced activation levels of all markers in ACC1 pKO perfused blood on both collagen surfaces (Figure 6A,E-G, supplemental Figure 5A,E-G), confirming the loss-of-function phenotype of ACC1 pKO platelets even under flow conditions simulating thrombus formation in a blood vessel.

In vivo thrombus growth in ACC1 pKO mice was impaired, without effect on hemostasis

Finally, we investigated the role of platelet ACC1 in physiological hemostasis and thrombosis using *in vivo* mouse models. First, a bleeding time assay was performed, showing that the average bleeding time in ACC1 pKO mice was similar to that of ACC1$^{flx/flx}$ and GPIbα-Cre$^{+/-}$ animals (Figure 7A). Next, we studied the involvement of platelet-specific ACC1 in arterial thrombus formation using the well-established carotid artery thrombosis model induced by ferric chloride.[40] Thrombus formation was monitored in real time by intravital fluorescence microscopy. In line with the impaired reactivity of ACC1-deficient platelets, thrombus growth was significantly reduced in ACC1 pKO mice compared with ACC1$^{flx/flx}$ mice (Figure 7B and 7D) and showed a moderate yet reproducible reduction when compared with GPIbα-Cre$^{+/-}$ controls (Figure 7C and 7D).

Discussion

Lipid metabolism in platelets has gained increasing attention in recent years, particularly regarding platelet activation and thrombotic diseases. Our previous research has demonstrated that systemic activation of ACC promotes platelet activation and thrombosis by extensively remodeling the platelet phospholipidome.[20] However, selective ACC1 deletion effects on lipid composition and function of platelets had not yet been explored. Using the newly developed GPIbα-Cre$^{+/-}$ mouse model[31], we provided definitive evidence that ACC1 is a crucial regulator of the platelet phospholipidome, with substantial implications for thrombus growth, as shown in both *in vivo* and *ex vivo* studies. This not only corroborates previous findings but also clearly indicates that ACC1 and lipid metabolism are key modulators of platelet function.

The GPIbα-Cre$^{+/-}$ model enables the selective deletion of the floxed ACC1 gene within the MK lineage, avoiding the off-target effects associated with PF4-Cre. PF4-Cre can exhibit leaky expression in non-megakaryocytic and even non-hematopoietic cells, particularly under inflammatory conditions, and has been linked to aberrant chemokine expression, which may confound phenotypic analyses [31, 41, 42]. GPIbα-Cre$^{+/-}$ mice display normal platelet function and hemostasis, with only minor changes in platelet volume and receptor expression.[31] Interestingly, ACC1 deficiency further increases MPV, potentially explaining, at least in part, the increased αIIbβ3 surface expression observed in ACC1 pKO platelets compared with GPIbα-Cre$^{+/-}$ and ACC1$^{flx/flx}$ control mice.[31, 43, 44] We also reported a significant platelet count reduction in ACC1pKO mice, consistent with findings in humans and primates following pharmacological ACC inhibition.[45] In these cases, reduced platelet counts have been linked to impaired DNL-dependent synthesis of saturated PC species in MKs, essential for the formation of the demarcation membrane during platelet biogenesis.[45] Since we also noticed a reduction in PC 16:0/16:0 and PC 16:0/18:0 in ACC1 pKO platelets, we can speculate that similar changes occur in MKs, potentially contributing to the decreased platelet counts in ACC1pKO mice. While CD36 has also been implicated in megakaryopoiesis [30, 32, 33], its

upregulation in ACC1-deficient platelets suggests it is unlikely to contribute to the platelet count reduction in this model.

Although the mild thrombocytopenia in ACC1 pKO mice (≈25% reduction relative to controls) could theoretically impact thrombus formation, previous studies have suggested otherwise. Bourne *et al.* demonstrated that C57BL/6 mice maintain thrombus formation despite an approximate 50% platelet reduction induced by GPIbα-depleting antibody treatment.[46] This indicates that the decreased thrombus formation observed in ACC1 pKO mice likely results from altered platelet function rather than from reduced platelet count. Supporting this, ACC1 deficiency led to a significant decrease in TxA_2 formation, resulting from the reduction in plasmalogens containing AA. This reduction was associated with impaired platelet activation, both *in vitro* after agonist stimulation and *ex vivo* in flow chamber studies. To assess whether defective aggregation in ACC1 pKO platelets could be rescued by a key secondary agonist, we co-stimulated thrombin-treated platelets with exogenous ADP. Aggregation remained impaired, indicating that deficient dense granule secretion is not solely responsible. Rather, changes in the phospholipidome may more broadly affect membrane organization, signaling, and metabolism. These alterations may increase membrane fluidity or expansion at baseline, thereby contributing to the larger surface area of ACC1-deficient platelets, while compromising the cytoskeletal remodeling required for full spreading upon activation.

As exogenous AA is typically incorporated into phospholipids through fatty acid remodeling rather than *de novo* synthesis, further investigation is needed to elucidate ACC1-dependent mechanisms involved in the specific remodeling of the platelet phospholipidome. One hypothesis is that ACC1 deficiency could disrupt transacylation reactions required for the proper AA distribution across phospholipid pools, a process mediated by CoA-independent transacylase transfering AA from diacyl PC to vinyl-ether species like PEP, which are key free AA reservoirs for eicosanoid synthesis.[17, 47] In support of this hypothesis, the reduction in PEP levels in ACC1 pKO platelets may reflect impaired ether lipid metabolism, which begins in peroxisomes. Although anucleate, platelets retain peroxisomal enzymes and express

PPARα, a regulator of peroxisome-related lipid pathways [48-51.] PE-plasmalogens support membrane architecture, oxidative homeostasis, and act as reservoirs for PUFAs like AA (TxA_2 precursor), and for PAF biosynthesis [52,53]. Therefore, ACC1 deletion may limit lipid substrates required for TxA_2 and PAF production, affecting platelet reactivity and inflammatory responses.

In addition to the reductions in saturated fatty acyl chains-containing PC and AA-containing PEP, we observed an increase in PUFAs within PC and PE classes. This pattern is consistent with findings in endothelial and cancer cells treated with ACC inhibitors, in which similar shifts in lipid composition have been linked to decreased membrane fluidity and integrity.[27-29] PUFA influence on plasma membrane organization has also been demonstrated in platelets.[1, 54] Moreover, PUFAs participate in thrombo-inflammatory signaling pathways.[55] Indeed, AA, DHA, and EPA serve as precursors for inflammatory lipid mediators. Thus, the up-regulation of PUFA-containing PC and PE in ACC1 pKO platelets is susceptible to influence thrombo-inflammatory responses, further highlighting the impact of ACC1 deficiency on platelet functions. Furthermore, ACC1 deficiency altered platelet sphingolipid content, primarily sphingomyelin (SM) and ceramide (CER), which together account for about 10-13% of the total dehydrated platelet mass.[56] Increased CER levels, while not directly impacting hemostasis or thrombosis, have been associated with pro-inflammatory cytokine secretion and enhanced P-selectin-mediated platelet-leukocyte aggregation.[57] Elevated CER levels in ACC1-deficient platelets might therefore contribute to a more inflammatory platelet profile, further supporting the role of ACC1 in modulating platelet-mediated inflammation.

Beyond lipid signaling, glycolysis is increasingly recognized as critical for platelet activation. Targeting metabolic enzymes such as pyruvate dehydrogenase kinases and pyruvate kinase M2 inhibits platelet activation and thrombosis by reducing aerobic glycolysis.[58-60] Our results suggest glycolytic impairment in ACC1-deficient platelets, both in basal and activated conditions, although the exact mechanism remains unclear. Interestingly, studies in yeast, liver cells, and cancer cells showed that ACC1 deficiency leads to protein hyperacetylation, including of histones, cytoskeletal, and metabolic proteins.[58-60] In line with this, our previous

work demonstrated that pharmacological ACC inhibition limits α-tubulin deacetylation upon thrombin stimulation, impairing platelet aggregation.[23] Future research should explore whether ACC1 deficiency affects glycolytic enzyme acetylation in platelets, with possible impacts on enzymatic activity and energy metabolism.

Regarding mitochondrial bioenergetics, ACC1 pKO platelets displayed unchanged basal and ATP-linked mitochondrial respiration but enhanced respiratory reserve capacity upon activation. This coincided with reduced PS exposure and protection against arterial thrombosis without impairing hemostasis. Notably, a similar phenotype occurs in 14-3-3ζ-deficient platelets[61], suggesting a shared mechanism. Although the link between ACC1 and respiratory reserve remains unclear, the enhancement may result from (i) increased endogenous substrate availability due to altered lipid metabolism, which may fuel the respiratory chain more effectively, and/or (ii) mitochondrial remodeling, involving specific phospholipids. It is well established that specific phospholipids are essential for mitochondrial function.[62, 63] For example, cardiolipin supports respiratory reserve in various cells by stabilizing the electron transport chain and optimizing electron flux under high-energy demands.[64, 65] Exploring a potential ACC1-cardiolipin interaction could offer insights into how ACC1 regulates platelet bioenergetics, procoagulant activity, and thrombosis. Finally, the enhanced respiratory capacity may also reflect a metabolic shift compensating for impaired lipogenesis. Platelets could rely more on glucose oxidation, CD36-mediated fatty acid uptake, or amino acid catabolism to sustain mitochondrial function, an area warranting future investigation through metabolic flux analysis.

In conclusion, our study highlights the critical role of ACC1 in platelet function through the regulation of specific phospholipid pools required for membrane architecture, activation, and energy metabolism. We demonstrate that ACC1 is a key regulator of thrombosis while maintaining baseline platelet reactivity which is essential for hemostasis. These findings provide a conceptual advance in understanding the physiological relevance of platelet ACC1 and establish this metabolic enzyme as a promising target for anti-thrombotic therapies.

Acknowledgments

The authors would like to thank Emmanuel Vandenhooft for his dedicated animal care.

This work was supported by grants from the Fonds National de la Recherche Scientifique et Médicale (FNRS, Brussels, Belgium, grant J.0150.18) and the Action de Recherche Concertée of the Wallonia-Brussels Federation, Brussels, Belgium (ARC 23/28-132). M.O. received support from the Fonds pour la formation à la Recherche dans l'Industrie et dans l'Agriculture (FRIA, Belgium) and a Bourse du Patrimoine (UCL, Belgium). L.P. and E.D. were supported by fellowships from the FNRS and FRIA, respectively. S.H. is an FNRS senior research associate.

Authorship Contributions

M.O. and L.P. performed the experiments, analyzed the data, wrote and edited the manuscript; E.D. wrote and edited the manuscript; A.M. performed the experiments, acquired and analyzed the data, especially for the arterial thrombosis studies; J.A. carried out the biostatistical and lipidomic data analysis; M.G. and B.G. performed the experiments, acquired and analyzed the data, especially for the lipidomic studies; A.G. and V.R. performed the experiments, acquired and analyzed the data, especially for flow cytometry analyses; M.K., C.Ba. and J.W.M.H. performed the experiments, acquired and analyzed the data, especially for the flow chambers studies; Z.N. and Y.S. generously provided the GpIbα-Cre animals mice; D.B. and C.Bo. provided experimental and conceptual advice on flow cytometry and immunohistochemistry experiments, respectively; L.B. secured funding, discussed results and their implications, and edited the manuscript; C.Be. conceived and designed the study, secured funding, discussed results and their implications and edited the manuscript. S.H. conceived and designed the study, secured funding, discussed results and their implications, wrote and edited the manuscript. All authors have read and approved the final manuscript before submission.

Conflict of Interest Disclosures

The authors declare no competing financial interests.

References

1. Harayama, T. and H. Riezman, *Understanding the diversity of membrane lipid composition.* Nat Rev Mol Cell Biol, 2018. **19**(5): p. 281-296.
2. Gruba, S.M., et al., *Platelet membrane variations and their effects on delta-granule secretion kinetics and aggregation spreading among different species.* Biochim Biophys Acta, 2015. **1848**(7): p. 1609-18.
3. Koseoglu, S., et al., *Analytical characterization of the role of phospholipids in platelet adhesion and secretion.* Anal Chem, 2015. **87**(1): p. 413-21.
4. Slatter, D.A., et al., *Mapping the Human Platelet Lipidome Reveals Cytosolic Phospholipase A2 as a Regulator of Mitochondrial Bioenergetics during Activation.* Cell Metab, 2016. **23**(5): p. 930-44.
5. Bettache, N., et al., *Mechanical constraint imposed on plasma membrane through transverse phospholipid imbalance induces reversible actin polymerization via phosphoinositide 3-kinase activation.* J Cell Sci, 2003. **116**(Pt 11): p. 2277-84.
6. Chicanne, G., et al., *What can we learn from the platelet lipidome?* Platelets, 2023. **34**(1): p. 2182180.
7. Chatterjee, M., *Platelet lipidome: Dismantling the "Trojan horse" in the bloodstream.* J Thromb Haemost, 2020. **18**(3): p. 543-557.
8. Duvernay, M.T., et al., *Platelet Lipidomic Profiling: Novel Insight into Cytosolic Phospholipase A2alpha Activity and Its Role in Human Platelet Activation.* Biochemistry, 2015. **54**(36): p. 5578-88.
9. Peng, B., et al., *Identification of key lipids critical for platelet activation by comprehensive analysis of the platelet lipidome.* Blood, 2018. **132**(5): p. e1-e12.
10. Lagoutte-Renosi, J., et al., *Influence of Antiplatelet Agents on the Lipid Composition of Platelet Plasma Membrane: A Lipidomics Approach with Ticagrelor and Its Active Metabolite.* Int J Mol Sci, 2021. **22**(3).

11. Rabani, V., et al., *Comparative lipidomics and proteomics analysis of platelet lipid rafts using different detergents.* Platelets, 2016. **27**(7): p. 634-641.
12. Rabani, V., et al., *Impact of ticagrelor on P2Y1 and P2Y12 localization and on cholesterol levels in platelet plasma membrane.* Platelets, 2018. **29**(7): p. 709-715.
13. Heimerl, S., et al., *Quantification of bulk lipid species in human platelets and their thrombin-induced release.* Sci Rep, 2023. **13**(1): p. 6154.
14. O'Donnell, V.B., R.C. Murphy, and S.P. Watson, *Platelet lipidomics: modern day perspective on lipid discovery and characterization in platelets.* Circ Res, 2014. **114**(7): p. 1185-203.
15. Watanabe, M., et al., *Relationship between platelet membrane lipid compositions and platelet aggregability in alcoholic liver disease.* Alcohol Clin Exp Res, 1998. **22**(S3 Pt 1): p. 97S-102S.
16. Beckett, C.S., et al., *Phospholipase A2-catalyzed hydrolysis of plasmalogen phospholipids in thrombin-stimulated human platelets.* Thromb Res, 2007. **120**(2): p. 259-68.
17. Perez-Chacon, G., et al., *Control of free arachidonic acid levels by phospholipases A2 and lysophospholipid acyltransferases.* Biochim Biophys Acta, 2009. **1791**(12): p. 1103-13.
18. Tsegaye, Y., K.O. Daasvatn, and H. Holmsen, *Acyl specificity of phospholipases A2 and C in thrombin-stimulated human platelets.* Platelets, 2002. **13**(1): p. 31-5.
19. Peng, B., et al., *Identification of key lipids critical for platelet activation by comprehensive analysis of the platelet lipidome.* Blood, 2018.
20. Lepropre, S., et al., *AMPK-ACC signaling modulates platelet phospholipids and potentiates thrombus formation.* Blood, 2018. **132**(11): p. 1180-1192.
21. Manke, M.C., R. Ahrends, and O. Borst, *Platelet lipid metabolism in vascular thrombo-inflammation.* Pharmacol Ther, 2022. **237**: p. 108258.
22. Okuma, M., S. Yamashita, and S. Numa, *Enzymic Studies on Phosphatidic Acid Synthesis in Human Platelets.* Blood, 1973. **41**(3): p. 379-389.

23. Octave, M., et al., *Acetyl-CoA Carboxylase Inhibitor CP640.186 Increases Tubulin Acetylation and Impairs Thrombin-Induced Platelet Aggregation.* Int J Mol Sci, 2021. **22**(23).
24. Gibson, D.M., E.B. Titchener, and S.J. Wakil, *Studies on the mechanism of fatty acid synthesis. V. Bicarbonate requirement for the synthesis of long-chain fatty acids.* Biochim Biophys Acta, 1958. **30**(2): p. 376-83.
25. Rowley, J.W., et al., *Genome-wide RNA-seq analysis of human and mouse platelet transcriptomes.* Blood, 2011. **118**(14): p. e101-11.
26. Yu, Y., et al., *Global analysis of the rat and human platelet proteome - the molecular blueprint for illustrating multi-functional platelets and cross-species function evolution.* Proteomics, 2010. **10**(13): p. 2444-2457.
27. Glatzel, D.K., et al., *Acetyl-CoA carboxylase 1 regulates endothelial cell migration by shifting the phospholipid composition.* J Lipid Res, 2018. **59**(2): p. 298-311.
28. Scott, K.E., et al., *Metabolic regulation of invadopodia and invasion by acetyl-CoA carboxylase 1 and de novo lipogenesis.* PLoS One, 2012. **7**(1): p. e29761.
29. Rysman, E., et al., *De novo lipogenesis protects cancer cells from free radicals and chemotherapeutics by promoting membrane lipid saturation.* Cancer Res, 2010. **70**(20): p. 8117-26.
30. Kelly, K.L., et al., *De novo lipogenesis is essential for platelet production in humans.* Nat Metab, 2020. **2**(10): p. 1163-1178.
31. Nagy, Z., et al., *The Gp1ba-Cre transgenic mouse: a new model to delineate platelet and leukocyte functions.* Blood, 2019. **133**(4): p. 331-343.
32. de Jonckheere, B., et al., *Critical shifts in lipid metabolism promote megakaryocyte differentiation and proplatelet formation.* Nat Cardiovasc Res, 2023. **2**: p. 835-852.
33. Valet, C., et al., *Adipocyte Fatty Acid Transfer Supports Megakaryocyte Maturation.* Cell Rep, 2020. **32**(1): p. 107875.
34. Ravi, S., et al., *Metabolic plasticity in resting and thrombin activated platelets.* PLoS One, 2015. **10**(4): p. e0123597.

562 35. Li, Z., et al., *Signaling during platelet adhesion and activation.* Arterioscler Thromb
563 Vasc Biol, 2010. **30**(12): p. 2341-9.
564 36. de Witt, S.M., et al., *Identification of platelet function defects by multi-parameter*
565 *assessment of thrombus formation.* Nat Commun, 2014. **5**: p. 4257.
566 37. Nagy, M., et al., *Comparative Analysis of Microfluidics Thrombus Formation in*
567 *Multiple Genetically Modified Mice: Link to Thrombosis and Hemostasis.* Front
568 Cardiovasc Med, 2019. **6**: p. 99.
569 38. Kuijpers, M.J., et al., *Complementary roles of glycoprotein VI and alpha2beta1*
570 *integrin in collagen-induced thrombus formation in flowing whole blood ex vivo.*
571 FASEB J, 2003. **17**(6): p. 685-7.
572 39. Brass, L.F., et al., *Hemostatic Thrombus Formation in Flowing Blood.* 2019: p. 371-
573 391.
574 40. Musumeci, L., et al., *Dual-specificity phosphatase 3 deficiency or inhibition limits*
575 *platelet activation and arterial thrombosis.* Circulation, 2015. **131**(7): p. 656-68.
576 41. Pertuy, F., et al., *Broader expression of the mouse platelet factor 4-cre transgene*
577 *beyond the megakaryocyte lineage.* J Thromb Haemost, 2015. **13**(1): p. 115-25.
578 42. Calaminus, S.D., et al., *Lineage tracing of Pf4-Cre marks hematopoietic stem cells*
579 *and their progeny.* PLoS One, 2012. **7**(12): p. e51361.
580 43. Khaspekova, S.G., et al., *Relationships of glycoproteins IIb-IIIa and Ib content with*
581 *mean platelet volume and their genetic polymorphisms.* Blood Coagul Fibrinolysis,
582 2014. **25**(2): p. 128-34.
583 44. Kunicki, T.J., et al., *Mean platelet volume and integrin alleles correlate with levels of*
584 *integrins alpha(IIb)beta(3) and alpha(2)beta(1) in acute coronary syndrome patients*
585 *and normal subjects.* Arterioscler Thromb Vasc Biol, 2012. **32**(1): p. 147-52.
586 45. Kelly, K.L., et al., *De novo lipogenesis is essential for platelet production in humans.*
587 Nat Metab, 2020.
588 46. Bourne, J.H., et al., *CLEC-2 Supports Platelet Aggregation in Mouse but not Human*
589 *Blood at Arterial Shear.* Thromb Haemost, 2022. **122**(12): p. 1988-2000.

47. Colard, O., M. Breton, and G. Bereziat, *Arachidonyl transfer from diacyl phosphatidylcholine to ether phospholipids in rat platelets.* Biochem J, 1984. **222**(3): p. 657-62.
48. Bentfeld-Barker, M.E. and D.F. Bainton, *Identification of primary lysosomes in human megakaryocytes and platelets.* Blood, 1982. **59**(3): p. 472-81.
49. Farstad, M., A.M. Bakken, and R.K. Berge, *The activity and subcellular distribution of the peroxisomal enzyme acyl-CoA oxidase in human blood platelets.* Biochem J, 1992. **286 (Pt 3)**(Pt 3): p. 829-31.
50. Hashizume, S., et al., *Activation of peroxisome proliferator-activated receptor alpha in megakaryocytes reduces platelet-derived growth factor-BB in platelets.* J Atheroscler Thromb, 2011. **18**(2): p. 138-47.
51. Tyagi, S., et al., *The peroxisome proliferator-activated receptor: A family of nuclear receptors role in various diseases.* J Adv Pharm Technol Res, 2011. **2**(4): p. 236-40.
52. Leidl, K., et al., *Mass spectrometric analysis of lipid species of human circulating blood cells.* Biochim Biophys Acta, 2008. **1781**(10): p. 655-64.
53. Ashraf, M.A. and V. Nookala, *Biochemistry of Platelet Activating Factor*, in *StatPearls*. 2025: Treasure Island (FL).
54. Shaikh, S.R., et al., *How polyunsaturated fatty acids modify molecular organization in membranes: insight from NMR studies of model systems.* Biochim Biophys Acta, 2015. **1848**(1 Pt B): p. 211-9.
55. Lu, Y., et al., *Mediator-lipidomics: databases and search algorithms for PUFA-derived mediators.* J Lipid Res, 2005. **46**(4): p. 790-802.
56. Dolegowska, B., A. Lubkowska, and L. De Girolamo, *Platelet lipidomic.* J Biol Regul Homeost Agents, 2012. **26**(2 Suppl 1): p. 23S-33S.
57. Zhang, X., et al., *Alkaline ceramidase 1-mediated platelet ceramide catabolism mitigates vascular inflammation and abdominal aortic aneurysm formation.* Nat Cardiovasc Res, 2023. **2**(12): p. 1173-1189.

58. Flora, G.D., et al., *Mitochondrial pyruvate dehydrogenase kinases contribute to platelet function and thrombosis in mice by regulating aerobic glycolysis.* Blood Adv, 2023. **7**(11): p. 2347-2359.
59. Nayak, M.K., et al., *Dichloroacetate, an inhibitor of pyruvate dehydrogenase kinases, inhibits platelet aggregation and arterial thrombosis.* Blood Adv, 2018. **2**(15): p. 2029-2038.
60. Nayak, M.K., et al., *The metabolic enzyme pyruvate kinase M2 regulates platelet function and arterial thrombosis.* Blood, 2021. **137**(12): p. 1658-1668.
61. Schoenwaelder, S.M., et al., *14-3-3zeta regulates the mitochondrial respiratory reserve linked to platelet phosphatidylserine exposure and procoagulant function.* Nat Commun, 2016. **7**: p. 12862.
62. Horvath, S.E. and G. Daum, *Lipids of mitochondria.* Prog Lipid Res, 2013. **52**(4): p. 590-614.
63. Joshi, A., T.H. Richard, and V.M. Gohil, *Mitochondrial phospholipid metabolism in health and disease.* J Cell Sci, 2023. **136**(17).
64. Marchetti, P., et al., *Mitochondrial spare respiratory capacity: Mechanisms, regulation, and significance in non-transformed and cancer cells.* FASEB J, 2020. **34**(10): p. 13106-13124.
65. Nguyen, H.M., et al., *Reduction in cardiolipin decreases mitochondrial spare respiratory capacity and increases glucose transport into and across human brain cerebral microvascular endothelial cells.* J Neurochem, 2016. **139**(1): p. 68-80.

Figure legends

Figure 1. Characterization of ACC1$^{flx/flx}$, GPIbα-Cre$^{+/-}$, and ACC1 pKO mice. (**A**) Washed murine platelets or leukocytes were lysed and subjected to western blot analysis for ACC1 and ACC2 expression. Liver extract was used as positive control for ACC2. GAPDH served as loading control for platelet, leukocyte, and liver samples. (**B and C**) Platelet counts and mean platelet volumes (MPV) were determined by Cell-Dyn Emerald Hematology Analyzer (Abbott) in a single measurement conducted during the usage period of mice (8–16 weeks old). Data are expressed as mean±SEM (n=at least 27). $^{\#}$p≤0.0001 relative to ACC1$^{flx/flx}$ mice, $^{\$}$p≤0.0001 relative to GPIbα-Cre$^{+/-}$ mice, and §p≤0.0001 between ACC1$^{flx/flx}$ and GPIbα-Cre$^{+/-}$ mice. One-way ANOVA was used for data analysis. (**D**) Alexa488-GPIbβ antibody was injected into ACC1$^{flx/flx}$, GPIbα-Cre$^{+/-}$, and ACC1 pKO mice to analyze platelet lifespan. Blood samples were collected on the day of the injection (day 0), as well as on days 3 and 5 post-injection. Platelets were stained ex vivo with PE-conjugated anti-CD41 antibody, and the percentage of Alexa488^{+} platelets among total CD41^{+} platelets was quantified by flow cytometry. Data are expressed as mean±SEM (n=at least 3). $^{\#}$p≤0.05 relative to ACC1$^{flx/flx}$ mice, $^{\$}$p≤0.01 relative to GPIbα-Cre$^{+/-}$ mice. Data were subjected to two-way ANOVA analysis. (**E**) Platelet surface expression of αIIbβ3, GPIbα, and GPVI was measured by flow cytometry and normalized to mean platelet volume (MPV). Data are expressed as median fluorescence intensity (MFI) adjusted to MPV (fL)±SEM (n=at least 8). $^{\#}$p≤0.05 relative to ACC1$^{flx/flx}$ mice, $^{\$}$p≤0.01 relative to GPIbα-Cre$^{+/-}$ mice, and §p≤0.01 between ACC1$^{flx/flx}$ and GPIbα-Cre$^{+/-}$ mice. Data were subjected to one-way ANOVA analysis. Abbreviation: GADPH = glyceraldehyde 3-phosphate dehydrogenase.

Figure 2. Lipidomic analysis revealed changes in lipid profiles of ACC1 pKO platelets. Lipid extraction was performed on washed murine platelets from six samples for one genotype, each sample consisting of platelets pooled from two or three mice of the same genotype. (**A**) Platelet lipidome overview of ACC1 pKO, and ACC1$^{flx/flx}$, and GPIbα-Cre$^{+/-}$ controls by principal component analysis (PCA). The colors and symbols distinguish the

three genotypes. The first and second dimensions with their associated percentage of explained variance are displayed on the x- and y-axes, respectively. (**B-F**) Lipidomic analysis comparing ACC1 pKO and ACC1$^{flx/flx}$ platelets. (**B**) Box and scatter plot representations of the modulation (log_2FC) of 446 identified lipid species categorized into five (sub)classes, each represented by a distinct color (red-FA; orange-GL; yellow-PL; green-SL; and blue-ST). Lipid species are represented as black or grey dots based on their statistical significance (black dots representing a significant adjusted p-value, FDR≤0.05, while grey dots correspond to FDR≥0.05). Lipids above the horizontal dotted line are up-regulated, while lipids below are down-regulated. Log fold-changes (FC) and FDR were calculated from the multivariate regression model. (**C-E**) Dot plots displaying the length and unsaturation levels of the two fatty acyl chains from PC (**C**), PE (**D**), and PEP (**E**). Color bars indicate the log fold-change from red (up-regulation) to blue (down-regulation). The adjusted p-value is represented by the circle diameter (the largest circle corresponds to FDR≤0.05). (**F**) Forest plot of AA-containing PC, PE, and PEP comparing ACC1$^{flx/flx}$ and ACC1 pKO mice. Data are presented as log fold-change (squares) relative to ACC1$^{flx/flx}$ platelets. (**G**) Radar plot showing the relative intensity of PC, PE, and PEP containing the 20:4 fatty acyl chains. The dark grey area corresponds to ACC1$^{flx/flx}$ mice, while the orange area corresponds to ACC1 pKO mice. Abbreviations: AA = arachidonic acid; CE = cholesterol ester; CER = ceramide; DG = diacylglycerol; FA = fatty acid; GL = glycerolipid ; HCER = hydroxyceramide; LPC = lysophosphatidylcholine; LPE = lysophosphatidylethanolamine; PA = phosphatidic acid; PC = phosphatidylcholine; PE = phosphatidylethanolamine; PEP = phosphatidylethanolamine plasmalogen; PG = phosphatidylglycerol; PI = phosphatidylinositol; PL = phospholipid; PS = phosphatidylserine; SL = sphingolipid; SM = sphingomyelin; ST = sterol; TG = triacylglycerol.

Figure 3. ACC1 deficiency in platelets had an impact on both mitochondrial reserve capacity and glycolytic activity. Oxygen consumption rates (OCR) was measured in washed murine platelets from ACC1$^{flx/flx}$ or pKO mice. (**A-B**) OCR was assessed under basal conditions, after stimulation with 1U/mL thrombin (Thr), and following sequential treatment

with 1µM oligomycin (O), 0.4µM carbonyl cyanide p-trifluoromethoxyphenylhydrazone (F), and a mix of 1µM antimycin A (AtA)/rotenone (R). (**A**) Representative OCR profiles are shown as mean±SEM (n=4). (**B**) Quantification of mitochondrial respiratory parameters including basal (baseline OCR – R/AtA sensitive OCR), thrombin (thrombin response - baseline OCR), ATP-linked (thrombin response - oligomycin sensitive OCR), maximal (FCCP sensitive – R/AtA sensitive OCR), reserve capacity (FCCP sensitive - thrombin responsive OCR), proton leak (oligomycin sensitive – R/AtA sensitive OCR), and non-mitochondrial (R/AtA sensitive OCR). Results are expressed as mean±SEM (n=4). (**C-D**) Extracellular acidification rate (ECAR), used as an indirect indicator of glycolytic activity, was measured in the same experimental conditions. (**C**) Representative ECAR profiles are shown as mean±SEM (n=4). (**D**) Quantification of basal and thrombin-induced ECAR. Results are expressed as mean±SEM (n=4). *p≤0.05 relative to unstimulated conditions. $^{\#}$p≤0.05 relative to ACC1$^{flx/flx}$ mice. Statistical analysis was performed using two-way ANOVA. Abbreviation: NS = non-stimulated**.**

Figure 4. ACC1 pKO platelets displayed reduced TxA_2 generation, dense granule secretion, and aggregation upon agonist stimulation. (**A-G**) Washed murine platelets from ACC1 floxed or pKO mice were stimulated with various thrombin (Thr) or collagen-related peptide (CRP) concentrations. (**A**) Platelets were stimulated with 100mU/mL Thr or 0.3µg/mL CRP for 5min, and TxB_2 was measured in the supernatant using an ELISA kit. Aspirin-treated platelets were included as a positive control for TxB_2 generation inhibition in the CRP condition. Data are expressed as mean±SEM (n=4). *p≤0.05 relative to unstimulated conditions. $^{\#}$p≤0.05 relative to ACC1$^{flx/flx}$ mice. Data were analyzed via two-way ANOVA. (**B**) Aggregation was analyzed by turbidimetry (Chrono-Log). Data are expressed as mean±SEM (n=at least 4). *p≤0.05 relative to the first agonist concentration. $^{\#}$p≤0.05 relative to ACC1$^{flx/flx}$ mice. Two-way ANOVA was used for analysis. (**C**) Aggregation profiles are shown. (**D**) Activated αIIbβ3 (JON/A) and (**E**) p-selectin (CD62P) exposure was detected by flow cytometry. Data are expressed as fold change±SEM (n=4) and mean±SEM (n=4)

respectively. *p≤0.05 relative to unstimulated conditions. #p≤0.05 relative to ACC1$^{flx/flx}$ mice. Two-way ANOVA was used for analysis. (**F**) Dense granule secretion was assessed via addition of luciferase-luciferin reagent (Chrono-log). Data are expressed as mean±SEM (n=at least 3). *p≤0.05 relative to the first agonist concentration. #p≤0.05 relative to ACC1$^{flx/flx}$ mice. Two-way ANOVA was used for analysis. (**G**) Profiles are shown.

Figure 5. Platelet-specific ACC1 deletion affects platelet spreading and actin cytoskeleton organization upon CRP stimulation. (A-E) Washed murine platelets were stimulated with or without CRP 0.3µg/mL for 30min. Platelets were stained with phalloidin-FITC for 45min at room temperature. **(A)** Panel of representative pictures. Scale bar, 5µm. **(B,C)** Quantification of the mean surface area covered by **(B)** unstimulated or **(C)** CRP-stimulated platelets independently of the platelet morphology. Data are expressed as mean±SEM (n=4). #p≤0.05 relative to ACC1$^{flx/flx}$ mice. Data underwent one-way ANOVA. **(D,E)** Proportion of the surface aera covered by **(D)** unstimulated or **(E)** CRP-stimulated platelets, being inactivated (discoid), extending filopodia, forming lamellipodia or fully spread after activation. Data are expressed as means ± SEM (n=4). #p≤0.05 relative to ACC1$^{flx/flx}$ mice. $p≤0.05 relative to GPIbCre$^{+/-}$ mice. Data underwent two-way ANOVA.

Figure 6. ACC1 deficiency in platelets impaired their activation and thrombus formation under flow conditions. (**A-G**) Whole blood from ACC1$^{flx/flx}$, GPIbα-Cre$^{+/-}$ and ACC1 pKO mice was perfused over collagen I-coated surface (50µg/mL) at a shear rate of 1,000s^{-1}. (**A**) Representative images of multilayered platelet thrombi (brightfield = BF), and activated αIIbβ3, CD62P, and phosphatidylserine (PS) stainings. (**B-D**) Platelet deposition, thrombus formation and contraction score were assessed on brightfield (BF) images. (**E**) αIIbβ3 activation was evaluated using JON/A Ab, (**F**) P-selectin exposure was evaluated via staining with anti-CD62P antibody, and (**G**) PS exposure was determined using annexin V. The results are expressed as mean±SEM (at least four mice/group). #p≤0.05 relative to ACC1$^{flx/flx}$ mice. $p≤0.05 relative to GPIbα-Cre$^{+/-}$ mice. One-way ANOVA was used for analysis.

Figure 7. ACC1 pKO mice exhibited reduced arterial thrombosis while maintaining normal hemostasis. (**A**) Tail bleeding times of $ACC1^{flx/flx}$, $GP1bCre^{+/-}$, and ACC1 pKO mice in saline solution preheated at 37°C. Results are expressed as mean±SEM (n=at least 23). Data were analyzed via one-way ANOVA. (**B-D**) Mice were subjected to thrombosis induced *in vivo* by $FeCl_3$ application to the carotid artery (10% of $FeCl_3$ during 5 minutes). Thrombus formation was visualized using intravital microscopy analyzing exogenous platelet accumulation stained with carboxyfluorescein succinimidyl ester (CFSE). (**B and C**) Thrombus growth area quantification over time. Data are expressed as mean±SEM (n=at least six). $^{\#}p \leq 0.05$ relative to $ACC1^{flx/flx}$ mice. Data were analyzed using unpaired t-test comparing AUC. (**D**) Representative pictures of thrombus formation over time (1, 5, 9, 15, and 19 minutes) after $FeCl_3$ injury.

Figure 1

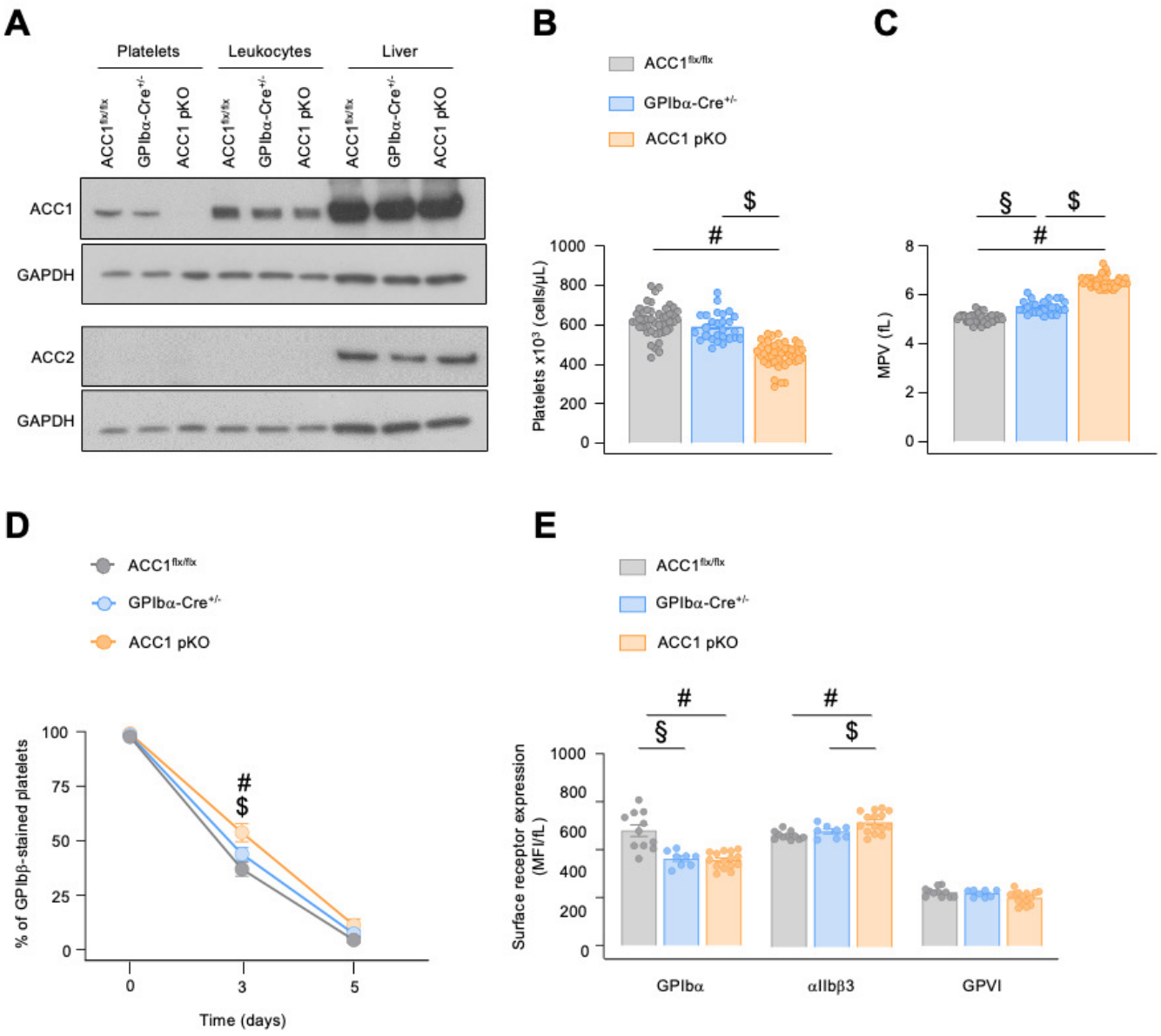
A
Platelets
Leukocytes
Liver
ACC1 pKO
ACC1
GAPDH
ACC2
GAPDH
B
GPIbα-Cre+/-
Platelets x10³ (cells/µL)
C
MPV (fL)
D
% of GPIbβ-stained platelets
Time (days)
E
Surface receptor expression (MFI/fL)
GPIbα
αIIbβ3
GPVI

Figure 2

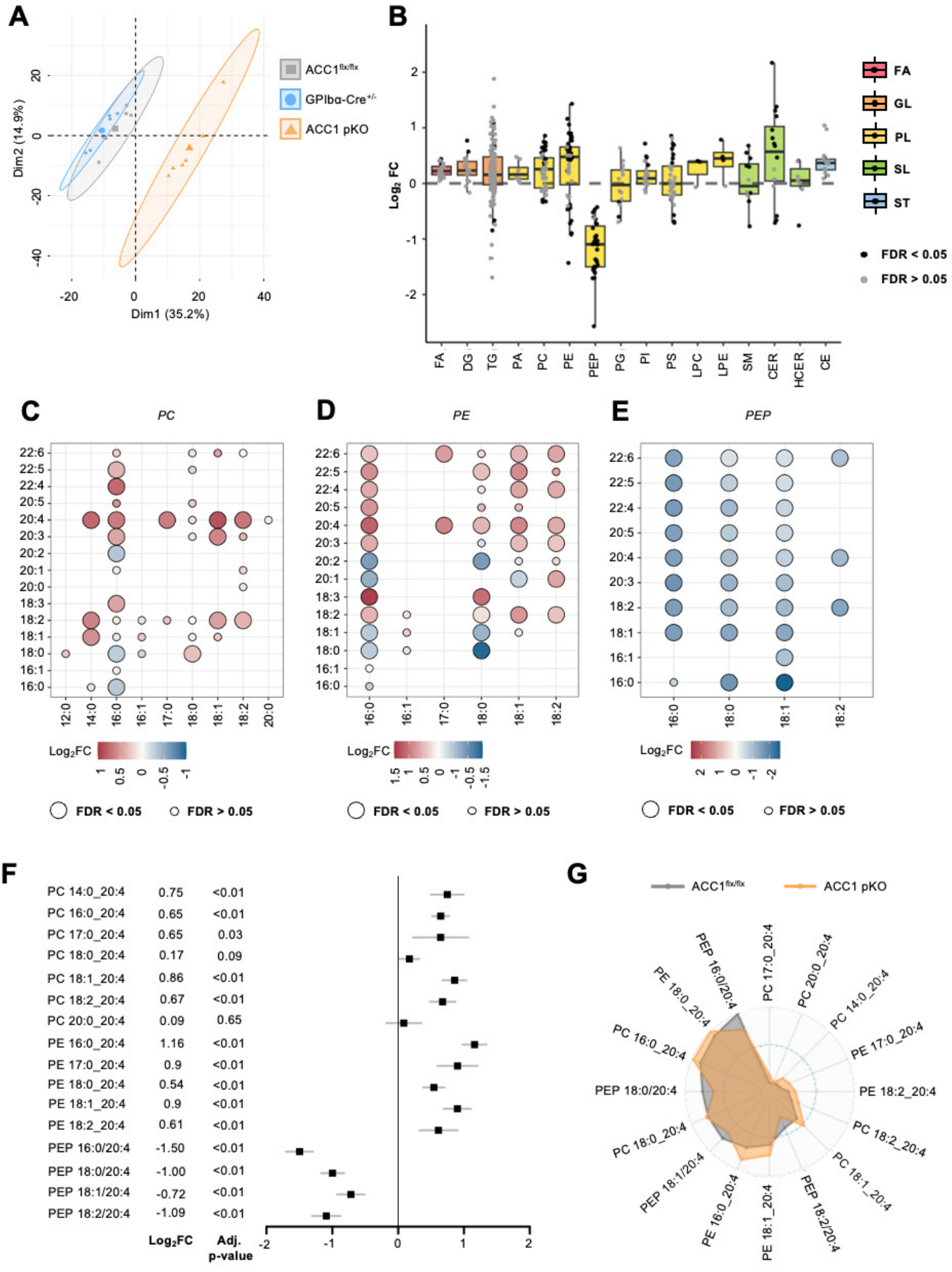
A
ACC1flx/flx
GPIbα-Cre+/-
ACC1 pKO
Dim2 (14.9%)
Dim1 (35.2%)
B
Log2 FC
FA
GL
PL
SL
ST
FDR < 0.05
FDR > 0.05
FA DG TG PA PC PE PEP PG PI PS LPC LPE SM CER HCER CE
C
PC
D
PE
E
PEP
Log2FC
FDR < 0.05
FDR > 0.05
F
PC 14:0_20:4 0.75 <0.01
PC 16:0_20:4 0.65 <0.01
PC 17:0_20:4 0.65 0.03
PC 18:0_20:4 0.17 0.09
PC 18:1_20:4 0.86 <0.01
PC 18:2_20:4 0.67 <0.01
PC 20:0_20:4 0.09 0.65
PE 16:0_20:4 1.16 <0.01
PE 17:0_20:4 0.9 <0.01
PE 18:0_20:4 0.54 <0.01
PE 18:1_20:4 0.9 <0.01
PE 18:2_20:4 0.61 <0.01
PEP 16:0/20:4 -1.50 <0.01
PEP 18:0/20:4 -1.00 <0.01
PEP 18:1/20:4 -0.72 <0.01
PEP 18:2/20:4 -1.09 <0.01
Log2FC
Adj. p-value
G
ACC1flx/flx
ACC1 pKO

Figure 3

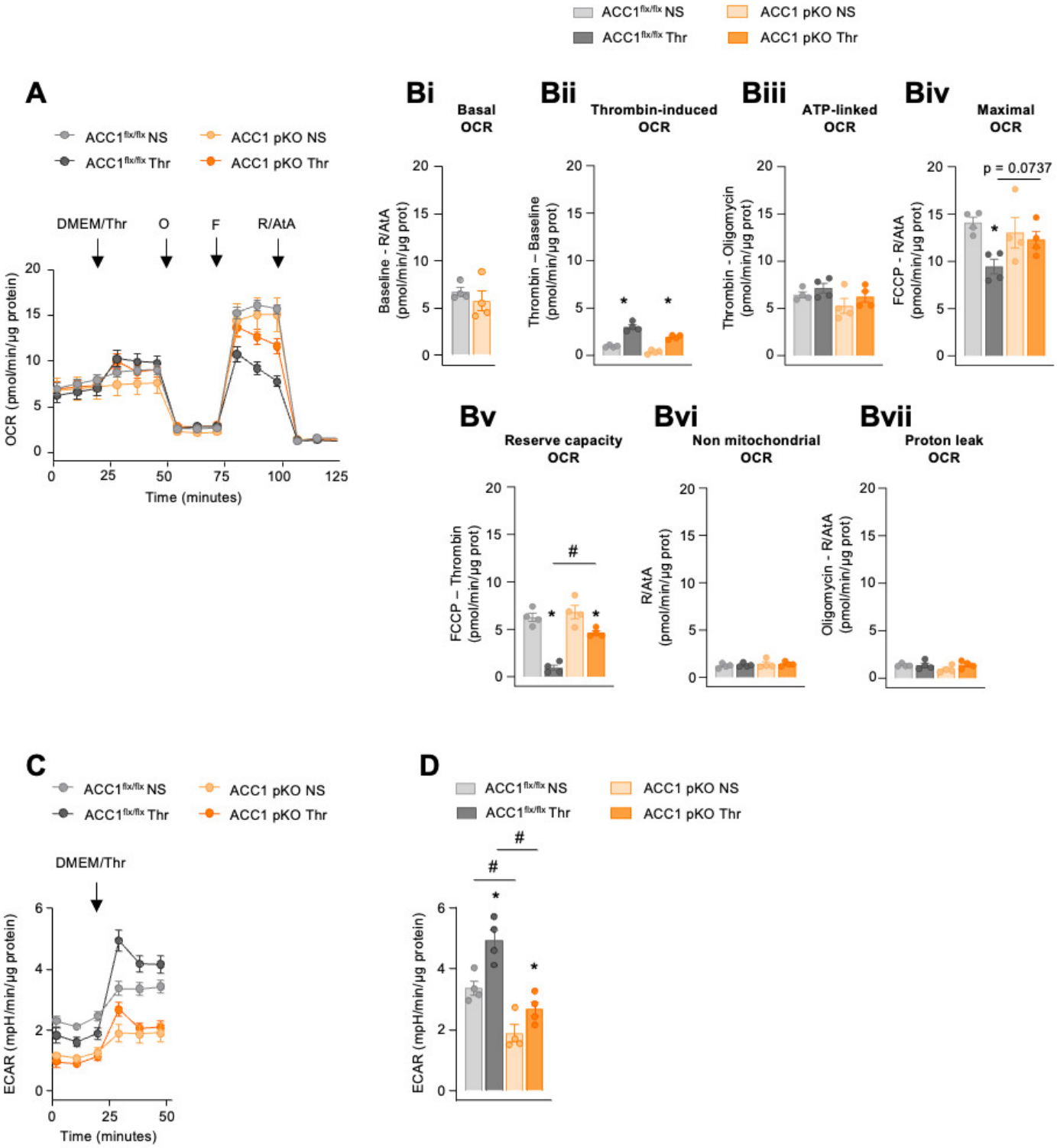
ACC1 flx/flx NS
ACC1 flx/flx Thr
ACC1 pKO NS
ACC1 pKO Thr
A
DMEM/Thr
O
F
R/AtA
OCR (pmol/min/µg protein)
Time (minutes)
Bi
Basal OCR
Baseline - R/AtA (pmol/min/µg prot)
Bii
Thrombin-induced OCR
Thrombin – Baseline (pmol/min/µg prot)
Biii
ATP-linked OCR
Thrombin - Oligomycin (pmol/min/µg prot)
Biv
Maximal OCR
p = 0.0737
FCCP - R/AtA (pmol/min/µg prot)
Bv
Reserve capacity OCR
FCCP – Thrombin (pmol/min/µg prot)
Bvi
Non mitochondrial OCR
R/AtA (pmol/min/µg prot)
Bvii
Proton leak OCR
Oligomycin - R/AtA (pmol/min/µg prot)
C
DMEM/Thr
ECAR (mpH/min/µg protein)
Time (minutes)
D
ECAR (mpH/min/µg protein)

Figure 4

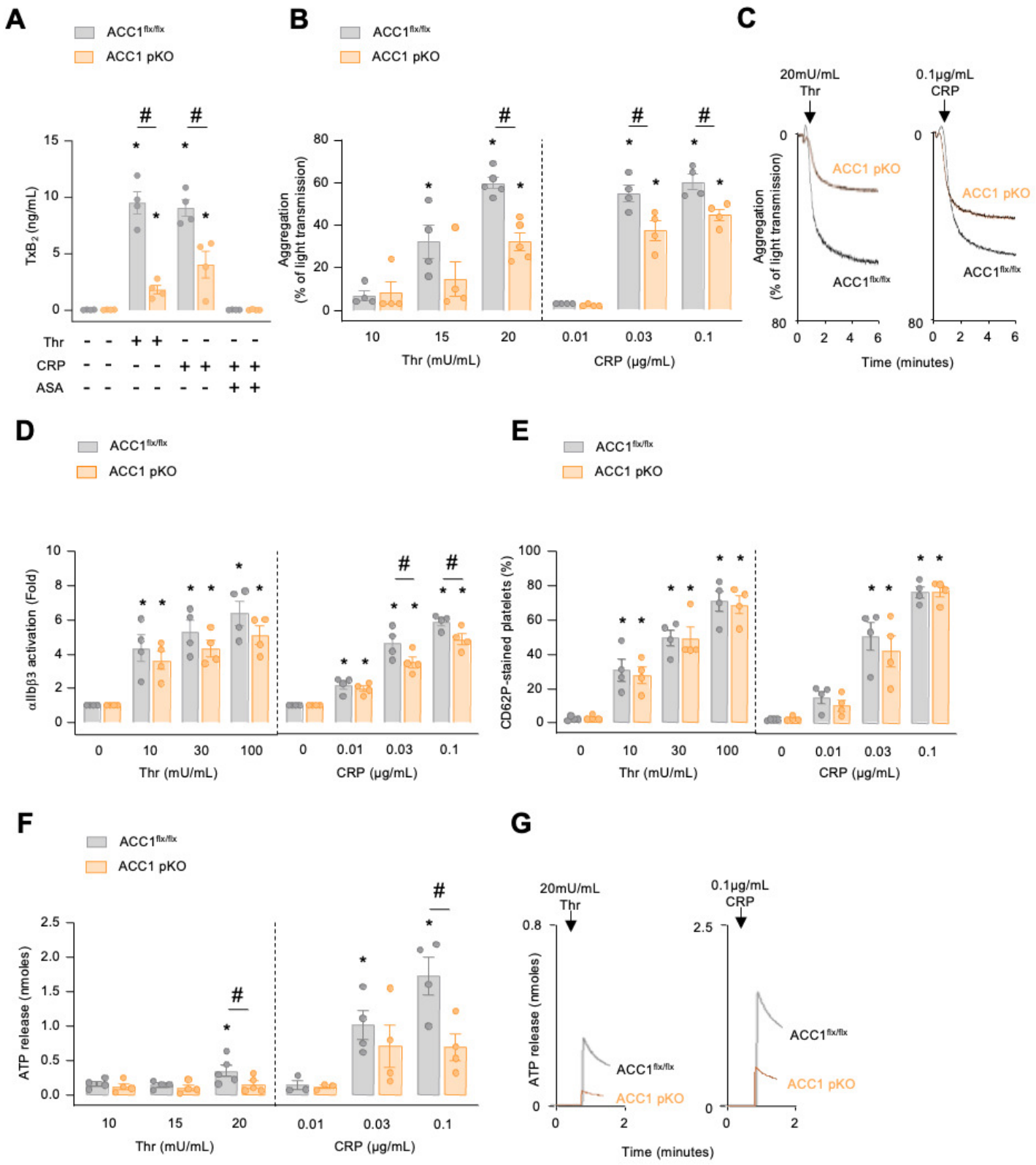
A
ACC1flx/flx
ACC1 pKO
TxB2 (ng/mL)
Thr
CRP
ASA
B
Aggregation (% of light transmission)
Thr (mU/mL)
CRP (µg/mL)
C
20mU/mL Thr
0.1µg/mL CRP
Aggregation (% of light transmission)
Time (minutes)
D
αIIbβ3 activation (Fold)
E
CD62P-stained platelets (%)
F
ATP release (nmoles)
G
ATP release (nmoles)
Time (minutes)

Figure 5

Figure 5

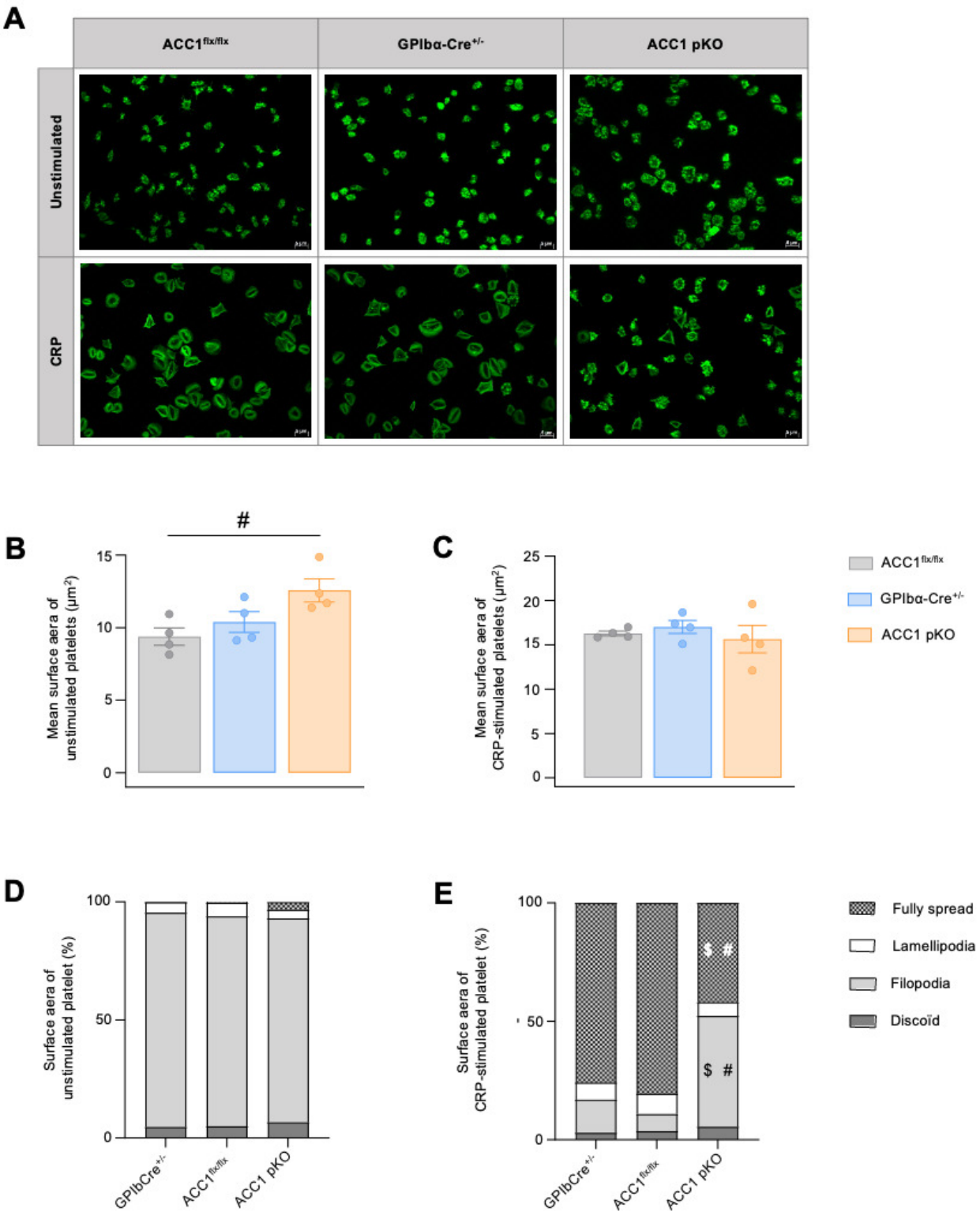

Figure 6

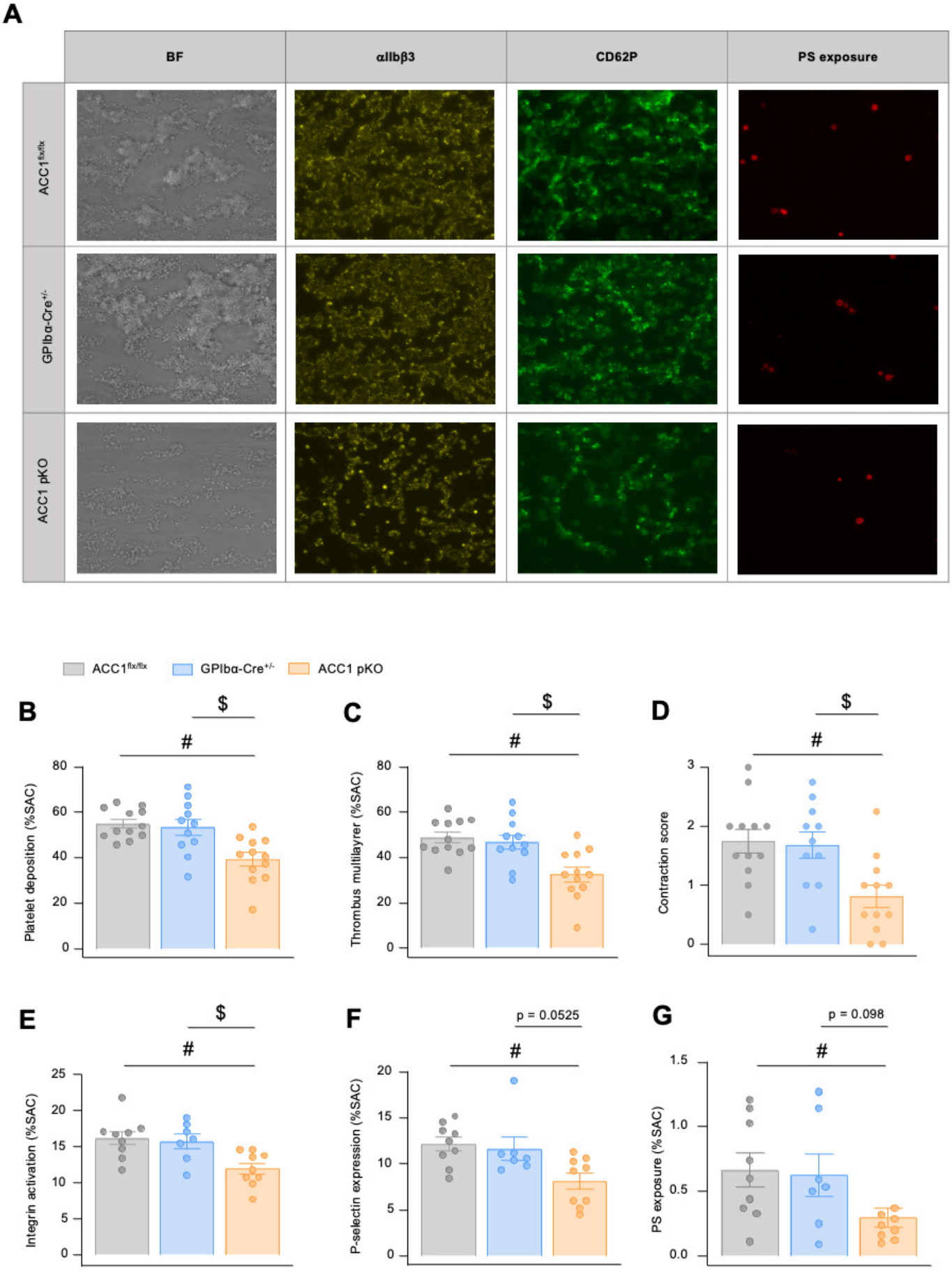
A
BF
αIIbβ3
CD62P
PS exposure
ACC1fix/fix
GPIbα-Cre+/-
ACC1 pKO
ACC1fix/fix
GPIbα-Cre+/-
ACC1 pKO
B
Platelet deposition (%SAC)
C
Thrombus multilayrer (%SAC)
D
Contraction score
E
Integrin activation (%SAC)
F
P-selectin expression (%SAC)
p = 0.0525
G
PS exposure (%SAC)
p = 0.098
$
#

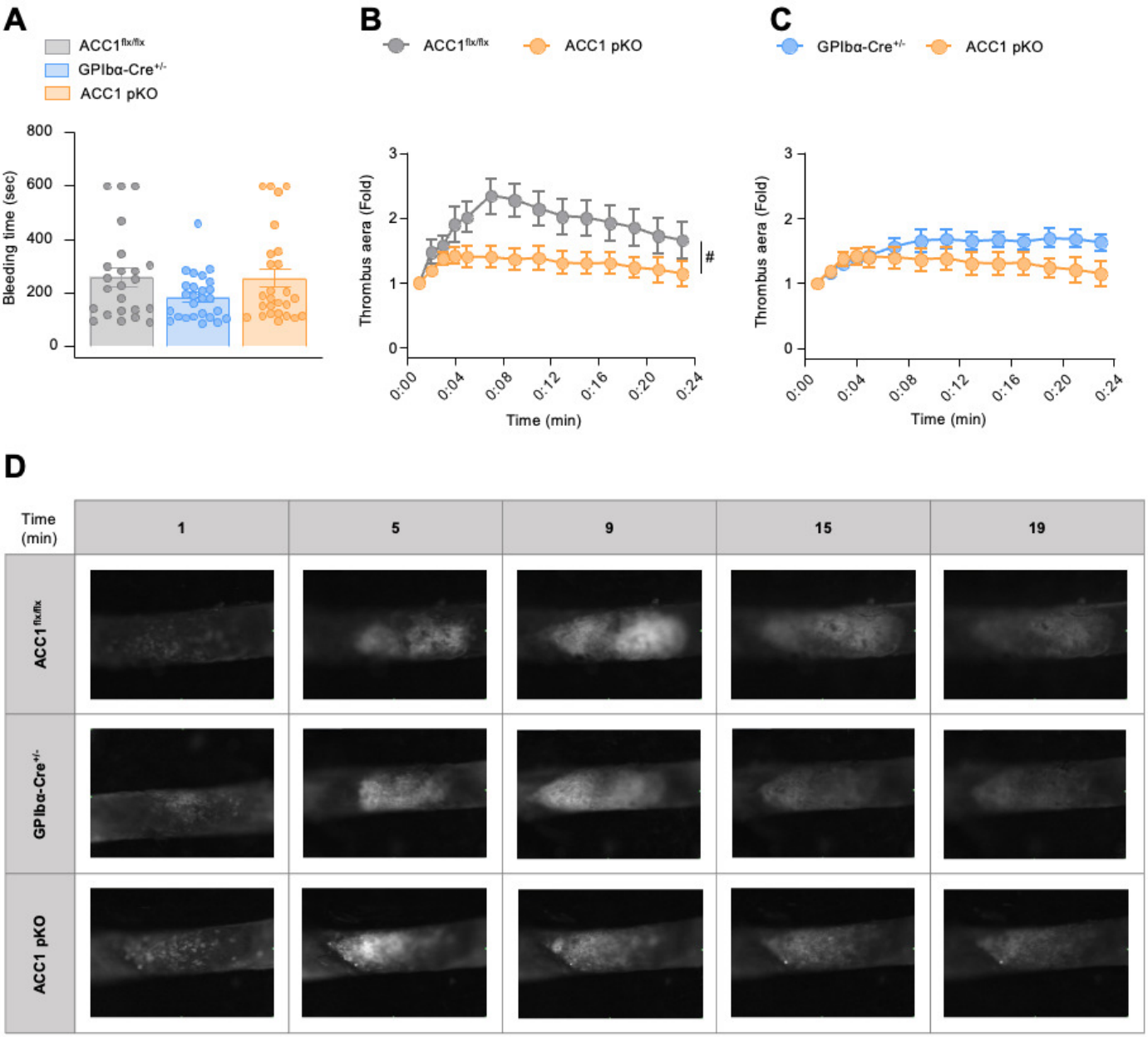
A
ACC1flx/flx
GPIbα-Cre+/-
ACC1 pKO
Bleeding time (sec)
800
600
400
200
0
B
ACC1flx/flx
ACC1 pKO
Thrombus aera (Fold)
3
2
1
0
#
0:00
0:04
0:08
0:12
0:16
0:20
0:24
Time (min)
C
GPIbα-Cre+/-
ACC1 pKO
Thrombus aera (Fold)
3
2
1
0
0:00
0:04
0:08
0:12
0:16
0:20
0:24
Time (min)
D
Time (min)
1
5
9
15
19
ACC1flx/flx
GPIbα-Cre+/-
ACC1 pKO